Research Article
Design of LQG Controller for Active Suspension without Considering Road Input Signals

Hui Pang, Ying Chen, JiaNan Chen, and Xue Liu

School of Mechanical and Precision Instrument Engineering, Xi'an University of Technology, Xi'an, Shaanxi, China

Correspondence should be addressed to Hui Pang; huipang@163.com

As the road conditions are completely unknown in the design of a suspension controller, an improved linear quadratic and Gaussian distributed (LQG) controller is proposed for active suspension system without considering road input signals. The main purpose is to optimize the vehicle body acceleration, pitching angular acceleration, displacement of suspension system, and tire dynamic deflection comprehensively. Meanwhile, it will extend the applicability of the LQG controller. Firstly, the half-vehicle and road input mathematical models of an active suspension system are established, with the weight coefficients of each evaluating indicator optimized by using genetic algorithm (GA). Then, a simulation model is built in Matlab/Simulink environment. Finally, a comparison of simulation is conducted to illustrate that the proposed LQG controller can obtain the better comprehensive performance of vehicle suspension system and improve riding comfort and handling safety compared to the conventional one.

1. Introduction

It is well known that vehicle suspension system plays a great role in evaluating vehicle dynamics performances including ride comfort, road handling, and suspension deflection. According to the different types of isolation components, the vehicle suspension systems are normally classified into three categories such as passive, semiactive, and active suspensions, which have been developed to improve vehicle ride comfort, handling stability, road damage minimization, and the overall vehicle dynamics performances [1]. In recent years, researchers have paid much more attention to study on the control approaches by considering the vibration problem of vehicle suspension system. The active suspension control method becomes a hot research topic in recent years, because the active suspension system can dynamically adjust the stiffness and damp of the suspension according to different driving conditions and can always reduce the vibration of vehicle suspension systems. The active suspension system mainly consists of actuator and control strategy, and as the actuator exports the control force fully in accordance with the requirements of the control strategy, the key of the controller design for active suspension is to select suitable control law which has good performance for the vehicle suspension.

Currently, the control strategies of active suspension system almost involve all the branches of control theory, such as sky-hook damper control theory [2–4], fuzzy logic control [5–7], backstepping control theory [8–11], and the LQG control theory [12–14], wherein the LQG control theory is widely used. Full state feedback and output feedback control laws are developed by using the conventional LQG control theory with its advantage being that all the vehicle states and outputs are fed back to the controller with detailed information. However, the road conditions are completely unknown in the design process of suspension controller [15]. Moreover, it is a big challenge in selecting the weight coefficients over the past decades [16]. In [17], the methodology of analytic hierarchy process (AHP) was used to determine the weight coefficients of performance indexes, which could enhance the effectiveness and accuracy for the design of LQG controller based on optimal control theory. Although the authors in [18] proposed an optimal design method of active suspension based on LQG control without road input signal, the selection of the weight coefficients was only used in quarter vehicle model, which may lead to the limitations to the practicality of the controller.

Therefore, it is necessary to simplify the controller design method and improve the applicability of the LQG controller
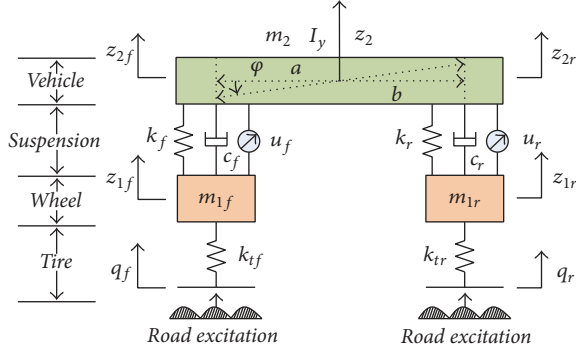
FIGURE 1: The active suspension dynamic model of half vehicle.

by ameliorating the conventional LQG controller. In this study, the partial state variable feedback technique is applied to develop an improved LQG controller for active suspension systems, in which the road input signals are ignored, whereby making it possible for extending the application area of LQG controller. Firstly, the half vehicle is taken as the research object and an improved LQG controller for active suspension without considering the road input signals is designed. Then, the optimization of the weight coefficients is conducted for the performance evaluation indicators such as the vehicle body acceleration, pitching angular acceleration, displacement of suspension system, and tire dynamic deflection, in which the GA is used to determine the weight coefficients of LQG controller. Finally, the comparisons of simulation analysis are addressed to verify the effectiveness and feasibility of the proposed LQG controller.

2. Modeling of Half-Vehicle Suspension Model and Rod Input Signals

2.1. Dynamic Model of Half-Vehicle Suspension System. The dynamic model of half-vehicle suspension system is used in this paper, and it is shown in Figure 1.

Based on the model in Figure 1 and Newtonian second law, the differential dynamics equations for passive suspension systems can be expressed as follows [19]:

$$
\begin{aligned}
&m_2\ddot{z}_2 + k_f\left(z_{2f} - z_{1f}\right) + c_f\left(\dot{z}_{2f} - \dot{z}_{1f}\right) + k_r\left(z_{2r} - z_{1r}\right) \\
&\quad + c_r\left(\dot{z}_{2r} - \dot{z}_{1r}\right) = 0, \\
&m_{1f}\ddot{z}_{1f} - k_f\left(z_{2f} - z_{1f}\right) - c_f\left(\dot{z}_{2f} - \dot{z}_{1f}\right) \\
&\quad + k_{tf}\left(z_{1f} - q_f\right) = 0, \\
&m_{1r}\ddot{z}_{1r} - k_r\left(z_{2r} - z_{1r}\right) - c_r\left(\dot{z}_{2r} - \dot{z}_{1r}\right) \\
&\quad + k_{tr}\left(z_{1r} - q_r\right) = 0, \\
&I_y\ddot{\varphi} - a\left[k_f\left(z_{2f} - z_{1f}\right) + c_f\left(\dot{z}_{2f} - \dot{z}_{1f}\right)\right] \\
&\quad + b\left[k_r\left(z_{2r} - z_{1r}\right) + c_r\left(\dot{z}_{2r} - \dot{z}_{1r}\right)\right] = 0.
\end{aligned}
\tag{1}
$$

Furthermore, the differential dynamics equations for active suspension systems can be written as follows [17]:

$$
\begin{aligned}
&m_2\ddot{z}_2 + k_f\left(z_{2f} - z_{1f}\right) + c_f\left(\dot{z}_{2f} - \dot{z}_{1f}\right) + u_f \\
&\quad + k_r\left(z_{2r} - z_{1r}\right) + c_r\left(\dot{z}_{2r} - \dot{z}_{1r}\right) + u_r = 0, \\
&m_{1f}\ddot{z}_{1f} - k_f\left(z_{2f} - z_{1f}\right) - c_f\left(\dot{z}_{2f} - \dot{z}_{1f}\right) - u_f \\
&\quad + k_{tf}\left(z_{1f} - q_f\right) = 0, \\
&m_{1r}\ddot{z}_{1r} - k_r\left(z_{2r} - z_{1r}\right) - c_r\left(\dot{z}_{2r} - \dot{z}_{1r}\right) - u_r \\
&\quad + k_{tr}\left(z_{1r} - q_r\right) = 0, \\
&I_y\ddot{\varphi} - a\left[k_f\left(z_{2f} - z_{1f}\right) + c_f\left(\dot{z}_{2f} - \dot{z}_{1f}\right) + u_f\right] \\
&\quad + b\left[k_r\left(z_{2r} - z_{1r}\right) + c_r\left(\dot{z}_{2r} - \dot{z}_{1r}\right) + u_r\right] = 0.
\end{aligned}
\tag{2}
$$

In fact, when the pitching angle of vehicle body around y-axis is too small, the displacements z_{2f} and z_{2r} at the two end points of the front and rear for the sprung mass can be approximately described as follows:

$$
\begin{aligned}
z_{2f} &\approx z_2 - z_{1f} - a\varphi, \\
z_{2r} &\approx z_2 - z_{1r} + b\varphi.
\end{aligned}
\tag{3}
$$

2.2. Modeling of Road Input Signals. The road profile of random white noise is first selected as excitation sources waveform for the front and rear wheel of vehicle suspension, and the mathematical formulas of road roughness are expressed as follows [20]:

$$
\begin{aligned}
\dot{q}_f &= -2\pi f_0 q_f + 2\pi\sqrt{G_0 v_0}\, w_1, \\
\dot{q}_r &= -2\pi f_0 q_r + 2\pi\sqrt{G_0 v_0}\, w_2.
\end{aligned}
\tag{4}
$$

However, for the half-vehicle mathematical model, the rear wheel is subjected to a certain delay of excitation relative to the front wheel that can be defined as $\tau = (a+b)/v_0$. In (4), q_f is the front road excitation; q_r is the rear road excitation; f_0 = 0.1 Hz is the cut-off frequency of road irregularity; G_0 is the coefficient of road irregularity. It is supposed that the vehicle speed v_0 = 20 m/s on grade B-class road, the coefficient of road irregularities $G_0 = 64 \times 10^3$ m^3, w_1 is the road profiles of front suspension system, and w_2 is the road profiles of rear suspension system. By using Matlab/Simulink software, the integral of white noise model is shown in Figure 2.

3. Optimal Design of the LQG Controller

3.1. The State-Space Equations of Passive and Active Suspension System. The main performance evaluation indicators in designing controller for half-vehicle active suspension are included as follows: (1) the vehicle body acceleration and the pitching angular acceleration evaluating the ride comfort and handing stability; (2) suspension dynamic deflection affecting the body posture; (3) tire dynamic deflection on behalf of
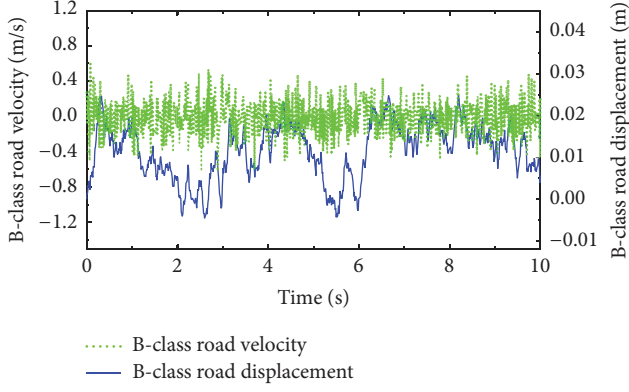
FIGURE 2: The road excitation used for simulation.

the tire road holding. Therefore, the state variable $\mathbf{X}$ and the output vector $\mathbf{Y}$ are selected as follows:

$$\mathbf{X} = \mathbf{Y}$$
$$= \left(z_{1f} \ \ q_f \ \ z_{1r} \ \ q_r \ \ z_{2f} - z_{1f} \ \ z_{2r} - z_{1r} \ \ \dot{z}_{1f} \ \ \dot{z}_{1r} \ \ \dot{z}_2 \ \ \dot{\varphi} \right)^T. \tag{5}$$

And then, by combining the differential equations of motion for passive and active suspension system of half-vehicle model with the road input equation, the state-space equations of passive and active suspension system can be described as formula (6) and formula (7):

$$\dot{\mathbf{X}} = \mathbf{A}_1 \mathbf{X} + \mathbf{B}_1 \mathbf{W},$$
$$\mathbf{Y} = \mathbf{C}\mathbf{X}, \tag{6}$$

$$\dot{\mathbf{X}} = \mathbf{A}_2 \mathbf{X} + \mathbf{B}_2 \mathbf{U} + \mathbf{F}\mathbf{W},$$
$$\mathbf{Y} = \mathbf{C}\mathbf{X}, \tag{7}$$

where $\mathbf{W}$ is the input matrix of white Gaussian noise expressed as the input matrix $\mathbf{W} = \begin{bmatrix} w_1 & w_2 \end{bmatrix}^T$, $\mathbf{U}$ is the input matrix of the active suspension expressed as $\mathbf{U} = \begin{bmatrix} u_f & u_r \end{bmatrix}^T$, and $\mathbf{C}$ is a 10×10 dimension unit matrix.

$$\mathbf{A}_1 = \begin{bmatrix}
0 & 0 & 0 & 0 & 0 & 0 & 1 & 0 & 0 & 0 \\
0 & -2\pi f_0 & 0 & 0 & 0 & 0 & 0 & 0 & 0 & 0 \\
0 & 0 & 0 & 0 & 0 & 0 & 0 & 1 & 0 & 0 \\
0 & 0 & 0 & -2\pi f_0 & 0 & 0 & 0 & 0 & 0 & 0 \\
0 & 0 & 0 & 0 & 0 & 0 & -2 & 0 & 1 & -a \\
0 & 0 & 0 & 0 & 0 & 0 & 0 & -2 & 1 & b \\
-\dfrac{k_{tf}}{m_{1f}} & \dfrac{k_{tf}}{m_{1f}} & 0 & 0 & \dfrac{k_f}{m_{1f}} & 0 & -\dfrac{2c_f}{m_{1f}} & 0 & \dfrac{c_f}{m_{1f}} & -\dfrac{ac_f}{m_{1f}} \\
0 & 0 & -\dfrac{k_{tr}}{m_{1r}} & \dfrac{k_{tr}}{m_{1r}} & 0 & \dfrac{k_r}{m_{1r}} & 0 & -\dfrac{2c_r}{m_{1r}} & \dfrac{c_r}{m_{1r}} & \dfrac{bc_r}{m_{1r}} \\
0 & 0 & 0 & 0 & -\dfrac{k_f}{m_2} & -\dfrac{k_r}{m_2} & \dfrac{2c_f}{m_2} & \dfrac{2c_r}{m_2} & -\dfrac{c_f + c_r}{m_2} & \dfrac{ac_f - bc_r}{m_2} \\
0 & 0 & 0 & 0 & \dfrac{ak_f}{I_y} & -\dfrac{bk_r}{I_y} & -\dfrac{2ac_f}{I_y} & \dfrac{2bc_r}{I_y} & \dfrac{ac_f - bc_r}{I_y} & -\dfrac{a^2 c_f + b^2 c_r}{I_y}
\end{bmatrix},$$

$$\mathbf{A}_2 = \mathbf{A}_1,$$

$$\mathbf{B}_1 = \mathbf{F} = \begin{bmatrix}
0 & 0 \\
2\pi \sqrt{G_0 v_0} & 0 \\
0 & 0 \\
0 & 2\pi \sqrt{G_0 v_0} \\
0 & 0 \\
0 & 0 \\
0 & 0 \\
0 & 0 \\
0 & 0 \\
0 & 0
\end{bmatrix},$$

$$\mathbf{B}_2 = \begin{bmatrix} 0 & 0 \\ 0 & 0 \\ 0 & 0 \\ 0 & 0 \\ 0 & 0 \\ 0 & 0 \\ \dfrac{1}{m_{1f}} & 0 \\ 0 & \dfrac{1}{m_{1r}} \\ -\dfrac{1}{m_2} & -\dfrac{1}{m_2} \\ \dfrac{a}{I_y} & -\dfrac{b}{I_y} \end{bmatrix}.$$

(8)

3.2. The Conventional LQG Controller.

When designing the LQG controller, it is necessary to consider all the performance evaluation indicators in order to achieve better comprehensive vehicle dynamics performance. So in this paper, the comprehensive performance evaluation indicator denoted by J is defined as follows [21, 22]:

$$J = \lim_{T \to \infty} \frac{1}{T} \int_0^T \left\{ q_1 a_z^2 + q_2 a a_z^2 + q_3 t_{df}^2 + q_4 t_{dr}^2 + q_5 f_{df}^2 \right.$$

$$+ q_6 f_{dr}^2 \right\} dt = \lim_{T \to \infty} \frac{1}{T} \int_0^T \left\{ q_1 \ddot{z}_2^2 + q_2 \ddot{\varphi}^2 \right.$$

$$+ q_3 \left(z_{1f} - q_f \right)^2 + q_4 \left(z_{1r} - q_r \right)^2 + q_5 \left(z_{2f} - z_{1f} \right)^2$$

$$\left. + q_6 \left(z_{2r} - z_{1r} \right)^2 \right\} dt,$$

(9)

where q_1, q_2, q_3, q_4, q_5, and q_6 are the weight coefficients of vehicle body acceleration, pitching angular acceleration, front and rear tire dynamic deflection, and displacement of front and rear suspension systems, respectively. Since it is of great importance for the vehicle body acceleration, the weight coefficient q_1 of the vehicle body acceleration is set to 1, which is used as a base value for the other coefficients to simplify the calculation.

Then formula (9) can be rewritten as an integral type of quadratic function by

$$J = \lim_{T \to \infty} \frac{1}{T} \int_0^T \left(X^T \mathbf{Q} X + U^T \mathbf{R} U + 2 X^T \mathbf{N} U \right) dt,$$

(10)

where

$$\mathbf{Q}$$

$$= \begin{bmatrix} q_3 & -q_3 & 0 & 0 & 0 & 0 & 0 & 0 & 0 & 0 \\ -q_3 & q_3 & 0 & 0 & 0 & 0 & 0 & 0 & 0 & 0 \\ 0 & 0 & q_4 & -q_4 & 0 & 0 & 0 & 0 & 0 & 0 \\ 0 & 0 & -q_4 & q_4 & 0 & 0 & 0 & 0 & 0 & 0 \\ 0 & 0 & 0 & 0 & \varepsilon_1 & \varepsilon_7 & \varepsilon_8 & \varepsilon_9 & \varepsilon_{10} & \varepsilon_{11} \\ 0 & 0 & 0 & 0 & \varepsilon_7 & \varepsilon_2 & \varepsilon_{12} & \varepsilon_{13} & \varepsilon_{14} & \varepsilon_{15} \\ 0 & 0 & 0 & 0 & \varepsilon_8 & \varepsilon_{12} & \varepsilon_3 & \varepsilon_{16} & \varepsilon_{17} & \varepsilon_{18} \\ 0 & 0 & 0 & 0 & \varepsilon_9 & \varepsilon_{13} & \varepsilon_{16} & \varepsilon_4 & \varepsilon_{19} & \varepsilon_{20} \\ 0 & 0 & 0 & 0 & \varepsilon_{10} & \varepsilon_{14} & \varepsilon_{17} & \varepsilon_{19} & \varepsilon_5 & \varepsilon_{21} \\ 0 & 0 & 0 & 0 & \varepsilon_{11} & \varepsilon_{15} & \varepsilon_{18} & \varepsilon_{20} & \varepsilon_{21} & \varepsilon_6 \end{bmatrix},$$

$$\mathbf{R} = \begin{bmatrix} \lambda_1 & \lambda_4 \\ \lambda_3 & \lambda_2 \end{bmatrix},$$

$$\mathbf{N} = \begin{bmatrix} 0 & 0 \\ 0 & 0 \\ 0 & 0 \\ 0 & 0 \\ \gamma_1 & \gamma_7 \\ \gamma_2 & \gamma_8 \\ \gamma_3 & \gamma_9 \\ \gamma_4 & \gamma_{10} \\ \gamma_5 & \gamma_{11} \\ \gamma_6 & \gamma_{12} \end{bmatrix}.$$

(11)

Among those matrices, the related variables are defined as follows:

$$\varepsilon_1 = \frac{k_f^2}{m_2^2} + \frac{q_2 a^2 k_f^2}{I_y^2} + q_5,$$

$$\varepsilon_2 = \frac{k_r^2}{m_2^2} + \frac{q_2 b^2 k_r^2}{I_y^2} + q_6,$$

$$\varepsilon_3 = \frac{4 c_f^2}{m_2^2} + \frac{4 q_2 a^2 c_f^2}{I_y^2},$$

$$\varepsilon_4 = \frac{4 c_r^2}{m_2^2} + \frac{4 q_2 b^2 c_r^2}{I_y^2},$$

$$\varepsilon_5 = \frac{(c_f + c_r)^2}{m_2^2} + \frac{q_2 (a c_f - b c_r)^2}{I_y^2},$$

$$\varepsilon_6 = \frac{(a c_f - b c_r)^2}{m_2^2} + \frac{q_2 (a^2 c_f + b^2 c_r)^2}{I_y^2},$$

$$\varepsilon_7 = \frac{k_f k_r}{m_2^2} - \frac{q_2 a b k_f k_r}{I_y^2},$$

$$\varepsilon_8 = -\frac{2 k_f c_f}{m_2^2} - \frac{2 q_2 a^2 k_f c_f}{I_y^2},$$

$$\varepsilon_9 = -\frac{2 k_f c_r}{m_2^2} + \frac{2 q_2 a b k_f c_r}{I_y^2},$$

$$\varepsilon_{10} = \frac{k_f (c_f + c_r)}{m_2^2} + \frac{q_2 a k_f (a c_f - b c_r)}{I_y^2},$$

$$\varepsilon_{11} = -\frac{k_f (a c_f - b c_r)}{m_2^2} - \frac{q_2 a k_f (a^2 c_f + b^2 c_r)}{I_y^2},$$

$$\varepsilon_{12} = -\frac{2 k_r c_f}{m_2^2} + \frac{2 q_2 a b k_r c_f}{I_y^2},$$

$$\varepsilon_{13} = -\frac{2 k_r c_r}{m_2^2} - \frac{2 q_2 b^2 k_r c_r}{I_y^2},$$

$$\varepsilon_{14} = \frac{k_r (c_f + c_r)}{m_2^2} - \frac{q_2 b k_r (a c_f - b c_r)}{I_y^2},$$

$$\varepsilon_{15} = -\frac{k_r (a c_f - b c_r)}{m_2^2} + \frac{q_2 b k_r (a^2 c_f + b^2 c_r)}{I_y^2},$$

$$\varepsilon_{16} = \frac{4 c_f c_r}{m_2^2} - \frac{4 q_2 a b c_f c_r}{I_y^2},$$

$$\varepsilon_{17} = -\frac{2 c_f (c_f + c_r)}{m_2^2} - \frac{2 q_2 a c_f (a c_f - b c_r)}{I_y^2},$$

$$\varepsilon_{18} = \frac{2 c_f (a c_f - b c_r)}{m_2^2} + \frac{2 q_2 a c_f (a^2 c_f + b^2 c_r)}{I_y^2},$$

$$\varepsilon_{19} = -\frac{2 c_r (c_f + c_r)}{m_2^2} + \frac{2 q_2 b c_r (a c_f - b c_r)}{I_y^2},$$

$$\varepsilon_{20} = \frac{2 c_r (a c_f - b c_r)}{m_2^2} - \frac{2 q_2 b c_r (a^2 c_f + b^2 c_r)}{I_y^2},$$

$$\varepsilon_{21} = -\frac{(c_f + c_r)(a c_f - b c_r)}{m_2^2} - \frac{q_2 (a c_f - b c_r)(a^2 c_f + b^2 c_r)}{I_y^2},$$

$$\lambda_1 = \frac{1}{m_2^2} + \frac{q_2 a^2}{I_y^2},$$

$$\lambda_2 = \frac{1}{m_2^2} + \frac{q_2 b^2}{I_y^2},$$

$$\lambda_3 = \lambda_4 = \frac{2}{m_2^2} - \frac{2 q_2 a b}{I_y^2},$$

$$\gamma_1 = \frac{k_f}{m_2^2} + \frac{q_2 a^2 k_f}{I_y^2},$$

$$\gamma_2 = \frac{k_r}{m_2^2} - \frac{q_2 a b k_r}{I_y^2},$$

$$\gamma_3 = -\frac{2 c_f}{m_2^2} - \frac{2 q_2 a^2 c_f}{I_y^2},$$

$$\gamma_4 = -\frac{2 c_r}{m_2^2} + \frac{2 q_2 a b c_r}{I_y^2},$$

$$\gamma_5 = c_f + \frac{c_r}{m_2^2} + \frac{q_2 a (a c_f - b c_r)}{I_y^2},$$

$$\gamma_6 = -a c_f - \frac{b c_r}{m_2^2} - \frac{q_2 a (a^2 c_f + b^2 c_r)}{I_y^2},$$

$$\gamma_7 = \frac{k_f}{m_2^2} - \frac{q_2 a b k_f}{I_y^2},$$

$$\gamma_8 = \frac{k_r}{m_2^2} + \frac{q_2 b^2 k_r}{I_y^2},$$

$$\gamma_9 = -\frac{2 c_f}{m_2^2} + \frac{2 q_2 a b c_f}{I_y^2},$$

$$\gamma_{10} = -\frac{2 c_r}{m_2^2} - \frac{2 q_2 b^2 c_r}{I_y^2},$$

$$\gamma_{11} = \frac{(c_f + c_r)}{m_2^2} - \frac{q_2 b (a c_f - b c_r)}{I_y^2},$$

$$\gamma_{12} = -\frac{(a c_f + b c_r)}{m_2^2} + \frac{q_2 b (a^2 c_f + b^2 c_r)}{I_y^2}.$$

(12)

Theoretically, the optimal control feedback gain matrix $\mathbf{K}$ that minimizes the desired vehicle performance index is a state feedback law $\mathbf{u} = -\mathbf{KX}$, whereby the feedback gain matrix $\mathbf{K}$ is determined by solving the following Riccati equation:

$$A\mathbf{K} + \mathbf{K}A^T + Q - \mathbf{K}BR^{-1}B^T\mathbf{K} + FWF^T = 0. \qquad (13)$$

However, it is impossible to obtain $\mathbf{K}$ before the vehicle parameters and the weight coefficients are determined. Then, according to the feedback state variables $\mathbf{X}$ at any time, the optimal control force of the actuator denoted by u_f and u_r can be described as follows:

$$\begin{bmatrix} u_f \\ u_r \end{bmatrix} = -\mathbf{KX}. \qquad (14)$$

The design of the improved LQG controller and the solving method of the weight coefficients will be discussed in the next section.

3.3. The Improved LQG Controller Design. The optimal feedback gain matrix $\mathbf{K}$ of LQG controller is described as follows:

$$\begin{aligned} \mathbf{K} &= R^{-1}\left(N^T + B^T P\right) \\ &= \begin{bmatrix} k_0 & k_1 & k_2 & k_3 & k_4 & k_5 & k_6 & k_7 & k_8 & k_9 \\ k_0' & k_1' & k_2' & k_3' & k_4' & k_5' & k_6' & k_7' & k_8' & k_9' \end{bmatrix}. \end{aligned} \qquad (15)$$

When the road input signals are not taken into consideration, the optimal control forces of u_f' and u_r' are described as formula (16):

$$\begin{aligned} \begin{bmatrix} u_f' \\ u_r' \end{bmatrix} &= -\mathbf{KX} \\ &= -\begin{bmatrix} k_0 & 0 & k_2 & 0 & k_4 & k_5 & k_6 & k_7 & k_8 & k_9 \\ k_0' & 0 & k_2' & 0 & k_4' & k_5' & k_6' & k_7' & k_8' & k_9' \end{bmatrix} \mathbf{X}. \end{aligned} \qquad (16)$$

In general case, the controllable effect of the LQG controller will be deteriorated if the optimal controllable forces u_f and u_r are directly changed to u_f' and u_r'. Therefore, it is necessary to optimize the control gain matrix $\mathbf{K}$ in order to improve the control performances of the active suspension, and it is then optimized into $\mathbf{K}_0$ for further development of the improved LQG controller as depicted in

$$\mathbf{K}_0 = \begin{bmatrix} k_{00} & 0 & k_{20} & 0 & k_{40} & k_{50} & k_{60} & k_{70} & k_{80} & k_{90} \\ k_{00}' & 0 & k_{20}' & 0 & k_{40}' & k_{50}' & k_{60}' & k_{70}' & k_{80}' & k_{90}' \end{bmatrix}. \qquad (17)$$

Meanwhile, according to the state-space equation of (6), the comprehensive performance evaluation indicator J of (7) and matrices $\mathbf{A}_2, \mathbf{B}_2, \mathbf{Q}, \mathbf{R}, \mathbf{N}$, the control gain matrix $\mathbf{K}$ can
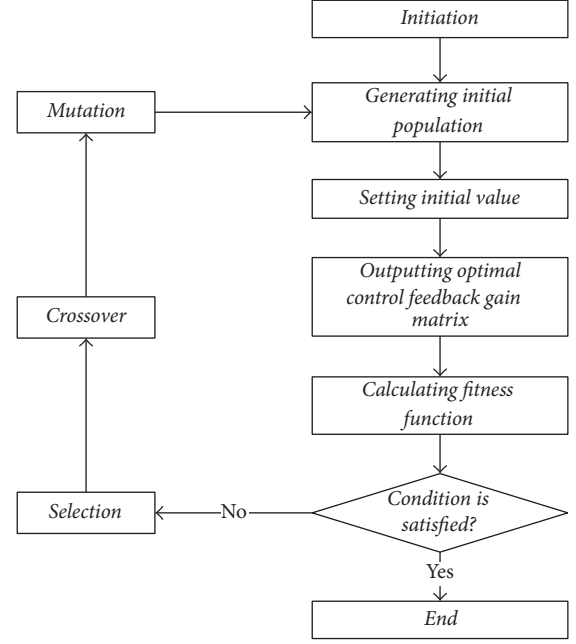

FIGURE 3: Flow chart for optimizing LQG controller based on GA.

be obtained with the help of Matlab software for the optimal linear quadratic controller. Thus, the design of the improved LQG controller is fulfilled. The main purpose of the optimization problem is to solve the weight coefficients of each performance evaluation indicator such as $q_1, q_2, q_3, q_4, q_5,$ and q_6.

Currently, most of the previous studies on the LQG controller design are usually focused on the selection of the weight coefficients by experts' experiences and random repeatable trials [23, 24]. Apparently, it is complex and uncontrollable process; the weight coefficients will not be changed once they are determined. Therefore, the adaptability of the optimal control algorithm is too limited. To overcome these disadvantages, the GA is applied to optimize the weight coefficients in the design of LQG controller in order to reduce the design time and avoid subjectivity. According to [25, 26], the flow chart for optimizing LQG controller based on GA is presented as shown in Figure 3.

Following the flow chart of LQG controller as shown in Figure 3, the detailed algorithm of developing the improved LQG controller is given as follows.

Step 1. Generate initial population.

Step 2. Assign each individual in the population to the weight coefficients $q_1, q_2, q_3, q_4, q_5,$ and q_6; in turn, the optimal control gain matrix $\mathbf{K}$ and the optimal control force can be obtained.

Step 3. Determine the fitness function values of each individual in the population.

Taking the differences between units and orders of magnitude of each of the performance evaluation indexes into

account, the fitness function L of the GA is set up as shown in

$$\min \quad L$$

$$= \frac{\text{RMS}\left[\ddot{z}_2\left(\mathbf{X}\right)\right]}{\text{RMS}\left[\ddot{z}_{2\text{pass}}\left(\mathbf{X}\right)\right]} + \frac{\text{RMS}\left[\ddot{\varphi}\left(\mathbf{X}\right)\right]}{\text{RMS}\left[\ddot{\varphi}_{\text{pass}}\left(\mathbf{X}\right)\right]}$$

$$+ \frac{\text{RMS}\left[\left(z_{1f} - q_f\right)\left(\mathbf{X}\right)\right]}{\text{RMS}\left[\left(z_{1f} - q_f\right)_{\text{pass}}\left(\mathbf{X}\right)\right]}$$

$$+ \frac{\text{RMS}\left[\left(z_{1r} - q_r\right)\left(\mathbf{X}\right)\right]}{\text{RMS}\left[\left(z_{1r} - q_r\right)_{\text{pass}}\left(\mathbf{X}\right)\right]}$$

$$+ \frac{\text{RMS}\left[\left(z_{2f} - z_{1f}\right)\left(\mathbf{X}\right)\right]}{\text{RMS}\left[\left(z_{2f} - z_{1f}\right)_{\text{pass}}\left(\mathbf{X}\right)\right]}$$

$$+ \frac{\text{RMS}\left[\left(z_{2r} - z_{1r}\right)\left(\mathbf{X}\right)\right]}{\text{RMS}\left[\left(z_{2r} - z_{1r}\right)_{\text{pass}}\left(\mathbf{X}\right)\right]} \tag{18}$$

$$\text{s.t.} \quad \frac{\text{RMS}\left[\ddot{z}_2\left(\mathbf{X}\right)\right]}{\text{RMS}\left[\ddot{z}_{2\text{pass}}\left(\mathbf{X}\right)\right]} < 1$$

$$\frac{\text{RMS}\left[\ddot{\varphi}\left(\mathbf{X}\right)\right]}{\text{RMS}\left[\ddot{\varphi}_{\text{pass}}\left(\mathbf{X}\right)\right]} < 1$$

$$\frac{\text{RMS}\left[\left(z_{1f} - q_f\right)\left(\mathbf{X}\right)\right]}{\text{RMS}\left[\left(z_{1f} - q_f\right)_{\text{pass}}\left(\mathbf{X}\right)\right]} < 1$$

$$\frac{\text{RMS}\left[\left(z_{1r} - q_r\right)\left(\mathbf{X}\right)\right]}{\text{RMS}\left[\left(z_{1r} - q_r\right)_{\text{pass}}\left(\mathbf{X}\right)\right]} < 1,$$

where RMS is the root mean square value for the population data; $\ddot{z}_{2\text{pass}}$ is the vehicle body acceleration value of passive suspension; $\ddot{\varphi}_{\text{pass}}$ is the pitching angular acceleration value of passive suspension; $(z_{1f} - q_f)_{\text{pass}}$, $(z_{1r} - q_r)_{\text{pass}}$ are the dynamic deflections of the front and rear tires for passive suspension, respectively; $(z_{2f} - z_{1f})_{\text{pass}}$, $(z_{2r} - z_{1r})_{\text{pass}}$ are the front and rear suspension deflections of passive suspension, respectively; $\mathbf{X}$ is the weight coefficient matrix.

Afterwards, the fitness function value is determined based on formula (17) with judging that whether the termination conditions of GA are satisfied. If it is satisfied, the algorithm is over; if not, it goes on for the last step and reselects the weight coefficients until it meets the requirements. Then it will go on for Step 4.

Step 4. The GA carries on the selection, crossover, and mutation and reserves the elites, generating new population and going on Step 2.

4. Numerical Examples and Discussion

In this section, in order to validate the effectiveness and correctness of the design procedure for the improved LQG

TABLE 1: Parameters of 4-DOF active suspension.

Parameters	Values
Sprung mass (m_2)	690 kg
Front unsprung mass (m_{1f})	40 kg
Rear unsprung mass (m_{1r})	45 kg
Damping coefficient of front suspension (c_f)	1000 N·s/m
Damping coefficient of rear suspension (c_r)	1000 N·s/m
Stiffness of front suspension (k_f)	17000 N/m
Stiffness of rear suspension (k_r)	22000 N/m
Stiffness of front tire (k_{tf})	200000 N/m
Stiffness of rear tire (k_{tr})	200000 N/m
Rotary inertia of vehicle body around y-axis (I_y)	1222 kg·m^2
Distance from the front axle to CG (a)	1.3 m
Distance from the rear axle to CG (b)	1.5 m

controller, a simulation example is presented to evaluate the proposed controller, that is, active suspension B with improved LQG controller, where active suspension A with conventional LQG controller and a passive suspension system are adopted for comparative analysis. The half-vehicle model parameters are listed in Table 1 for the following controller design [27]. It is just here to assume that the maximum allowable suspension displacement is $D_{\max} = \pm0.05$ m, and that the maximum value of controllable force is $F_{\max} = \pm500$ N.

Analytic hierarchy process (AHP) is a multicriteria decision aiding method based on a solid axiomatic foundation in which the general weight coefficient of each performance evaluation indicator related to ride comfort and handing stability can be obtained based on the objective and subjective weight proportion coefficients [17]. According to the computation progress based on AHP [22], the weight coefficients of each performance evaluation indicator are initially determined as $q_1 = 1$, $q_2 = 5.3$, $q_3 = 146032.8$, $q_4 = 102510.9$, $q_5 = 1065.8$, and $q_6 = 1207.8$. Therefore, to accelerate the convergence of GA, the initial search scope for each coefficient is defined as follows which is based on the results of AHP method; that is, the search scope of q_1 is set as $[1 \ \ 1]$, the search scope of q_2 is set as $[0.5 \ \ 10]$, the search scope of q_3 is set as $[10000 \ \ 200000]$, the search scope of q_4 is set as $[10000 \ \ 200000]$, the search scope of q_5 is set as $[500 \ \ 3000]$, and the search scope of q_6 is set as $[500 \ \ 3000]$. The filtered white noise is used as the road input model in the simulation calculation. The generation of white noise can be obtained by calling the function $WAG(M, N, P)$ with the help of Matlab software, in which M is the number of the rows for generating matrix, N is the number of columns, and P is the power of white noise and its unit is dB. In this paper, we choose $M = 2001$, $N = 1$, and $P = 20$ and choose 2001 sampling points in total, with the sampling time set to 0.005 s. When the vehicle speed is 20 m/s, the simulation road length is 2000 meters.

TABLE 2: Comparison of the root mean square values for each performance indicators.

Indicators	RMS			Effects (%) (+ deterioration, − improvement)		
	Passive suspension	Active suspension A	Active suspension B	Passive suspension	Active suspension A	Active suspension B
a_z (m/s^2)	0.0238	0.0103	0.0130	—	−56.7	−45.4
aa_z (rad/s^2)	0.0077	0.0027	0.0020	—	−64.9	−74.0
t_{df} (mm)	0.044	0.021	0.027	—	−52.3	−38.6
t_{dr} (mm)	0.046	0.019	0.023	—	−58.7	−50.0
f_{df} (mm)	0.47	1.00	1.20	—	+112.8	+155.3
f_{dr} (mm)	0.39	0.91	0.71	—	+133.3	+82.1
u_f (N)	—	110.8	91.8	—	—	—
u_r (N)	—	127.9	81.0	—	—	—

In order to obtain the optimal weight coefficients of each performance evaluation indicator for the LQG controller, the corresponding weight coefficients are calculated as $q_1 = 1$, $q_2 = 6.4$, $q_3 = 60105.7$, $q_4 = 30529.4$, $q_5 = 1499.2$, and $q_6 = 1347.6$ by using the GA. Thus, the optimal control gain matrix $\mathbf{K}$ is obtained as follows:

$$\mathbf{K} = \begin{bmatrix} 8865 & 0 & -3129 & 0 & 1878 & -4309 & -672 & 273 & -2846 & 2202 \\ 12541 & 0 & -8646 & 0 & -4822 & 9454 & 453 & -1077 & -2385 & -1605 \end{bmatrix}. \tag{19}$$

The simulation results for active suspension A, active suspension B, and passive suspension are, respectively, presented in Figure 4, which are, respectively, the responses to vehicle body acceleration, pitching angular acceleration, displacement of front/rear suspension systems, and front/rear tire dynamic deflection under the random road excitation with input time-delay $\tau = (a + b)/v_0$.

From Figure 4(a), it is seen that the active suspension A can remarkably reduce vehicle body acceleration in contrast with the other two suspension systems. From Figure 4(b), it is observed that the active suspension B can reduce pitching angular acceleration more greatly than active suspension A and passive suspension. From Figures 4(c) and 4(d), it is seen that the displacement of front/rear suspension systems are controlled in the scope of the design requirements ($D_{max} = \pm 50$ mm). In addition, it is seen from Figures 4(e) and 4(f) that the active suspension B can remarkably reduce tire dynamic deflection in contrast with the other two suspension systems.

Besides, the control forces for active suspension B are exhibited in Figure 5. It can be seen from Figures 5(a) and 5(b) that the allowable controllable force is within the control of actuator ($F_{max} = \pm 500$ N). With taking the effect of the front and rear suspension control forces into consideration, the active suspension with the proposed LQG controller can effectively reduce vibration transmission from uneven roads to the vehicle body. Therefore, the active suspensions can availably depress values of vehicle body acceleration, pitching angular acceleration, displacement of suspension system, and tire dynamic deflection in contrast with passive suspension.

Moreover, the vehicle active suspension with the proposed LOG controller can significantly improve ride comfort and handing stability.

To further conduct the simulation analysis in frequency domain, the power spectral density (PSD) response to vehicle body acceleration, pitching angular acceleration, displacement of front/rear suspension systems, and front/rear tire dynamic deflection are presented in Figure 6.

From Figure 6, it can be illustrated that a good control effect of the active suspension is achieved in the finite low frequency in contrast with the passive suspension, which indicates that the ride comfort and road handling are improved. Meanwhile, the amplitudes of PSD responses to vehicle body acceleration, pitching angular acceleration, displacement of suspension system, and tire dynamic deflection shows that there are almost not any changes in high frequency.

Additionally, to further demonstrate the effectiveness of the proposed LQG controller, the RMS values of the responses to vehicle body acceleration, pitching angular acceleration, displacement of suspension system, and tire dynamic deflection are listed in Table 2. Note that the percentage numbers in ratio line indicate the improvement of the proposed LQG controller compared with the conventional LQG controller and the passive suspension case under the same situations.

From Table 2, it is shown that both of the two active suspension systems can reduce vehicle body acceleration, pitching angular acceleration, and tire dynamic deflection remarkably in contrast with the passive one. The RMS values of vehicle body acceleration represented as a_z, pitching
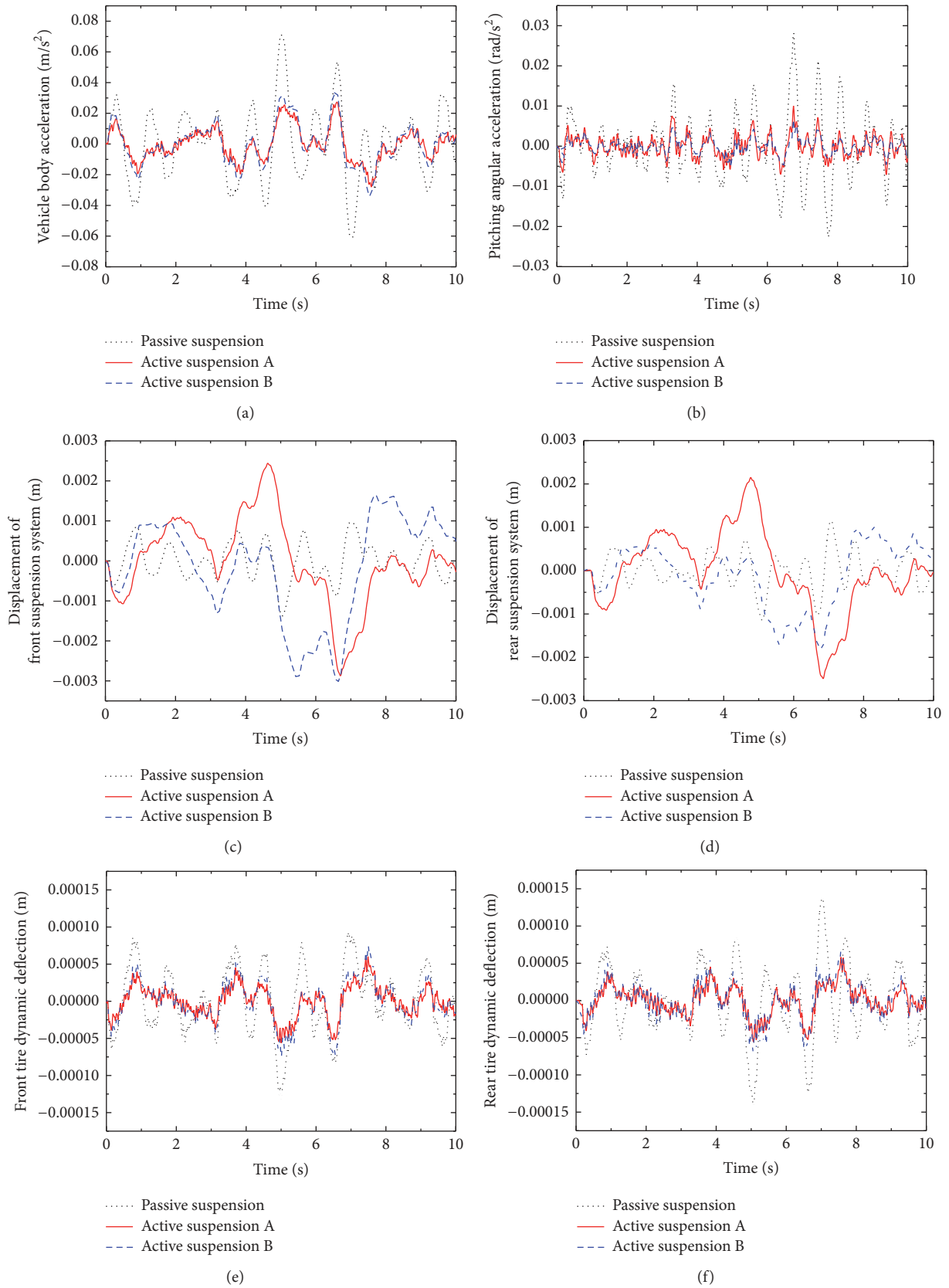
FIGURE 4: Time responses to passive suspension, active suspension A, and active suspension B.
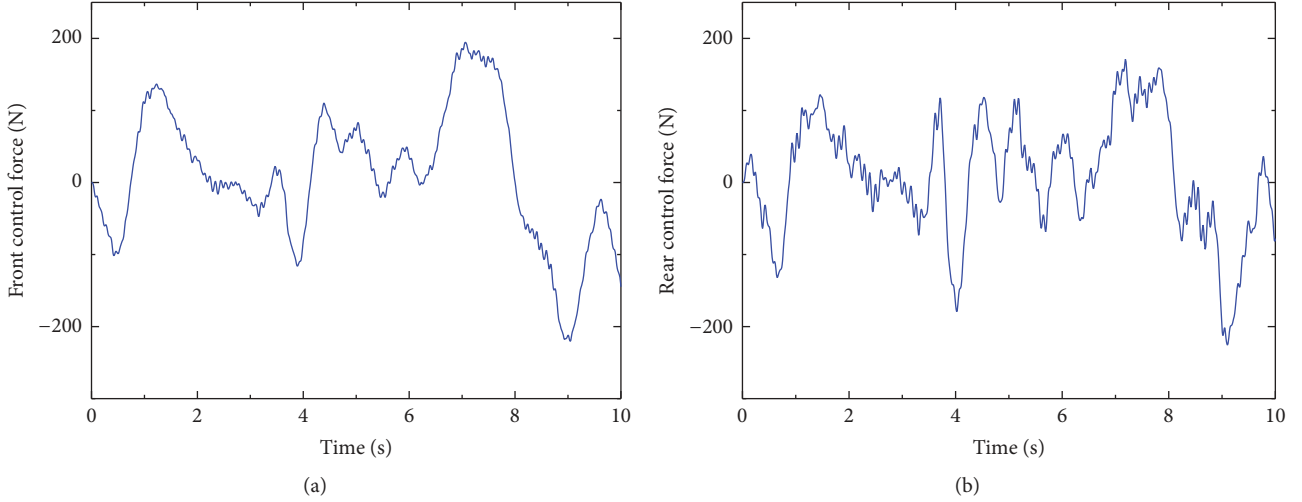
FIGURE 5: Simulation results of the active controllable force for the front and rear suspension.

angular acceleration represented as aa_z, and front/rear dynamic deflection denoted by t_{df}/t_{dr} for active suspension A are, respectively, reduced by 56.7%, 64.9%, 52.3%, and 58.7%, while the RMS values of the corresponding a_z, aa_z, t_{df}, and t_{dr} for active suspension B are, respectively, reduced by 45.4%, 74.0%, 38.6%, and 50.0%. Apparently, the two LQG controllers can significantly improve ride comfort and road holding. However, the road conditions are normally unknown in designing vehicle suspension controller (active suspension A); and it is difficult to measure the road surface signals constantly in designing a conventional LQG controller. Yet the road input signals can be neglected for the proposed LQG controller (active suspension B), which demonstrates that the improved LQG controller is more applicable than the conventional one.

5. Conclusion

(1) Taking the active suspension system of the half vehicle with four DOFs as a research objective, an improved LQG controller for active suspension system without considering road input signals is proposed to attain the comprehensive optimization of vehicle body acceleration, pitching angular acceleration, the front and rear dynamic deflection, and suspension deflection, which can further enhance the comprehensive performance of active suspension system.

(2) By considering that the road conditions are completely unknown in designing vehicle suspension controller, the improved LQG controller for active suspension systems is developed by using the partial state feedback control strategy, whereby ignoring the road input signals. And then, the optimal control feedback gain matrix is obtained based on the optimization of the weight coefficients for each evaluating indicator by using GA.

(3) A simulation model for the improved LQG controller of vehicle active suspension is built to verify the effectiveness and feasibility of the controller. The simulation result illustrates that using the LQG controller for active suspension without considering road input signals can improve the comprehensive performance of suspension system effectively and the riding comfort and handling safety.

(4) Future interesting and challenging research work will focus on establishing the test rig and developing the proposed LQG controller based on magnetorheological damper for the half-vehicle dynamics model, wherein the road input signals are not taken into account. Meanwhile, the stability analysis on the partial state variable feedback controller will be paid more consideration to further improve the controller performance.

Nomenclature

z_2: Displacement of vehicle body
z_{2f}: Displacement of the front sprung mass
z_{2r}: Displacement of the rear sprung mass
z_{1f}: Displacement of the front unsprung mass
z_{1r}: Displacement of the rear unsprung mass
q_f: Front road excitation
q_r: Rear road excitation
m_2: Sprung mass
m_{1f}: Front unsprung mass
m_{1r}: Rear unsprung mass
c_f: Damping coefficient of front suspension
c_r: Damping coefficient of rear suspension
k_f: Stiffness of front suspension
k_r: Stiffness of rear suspension
k_{tf}: Stiffness of front tire
k_{tr}: Stiffness of rear tire
I_y: Rotary inertia of vehicle body around y-axis
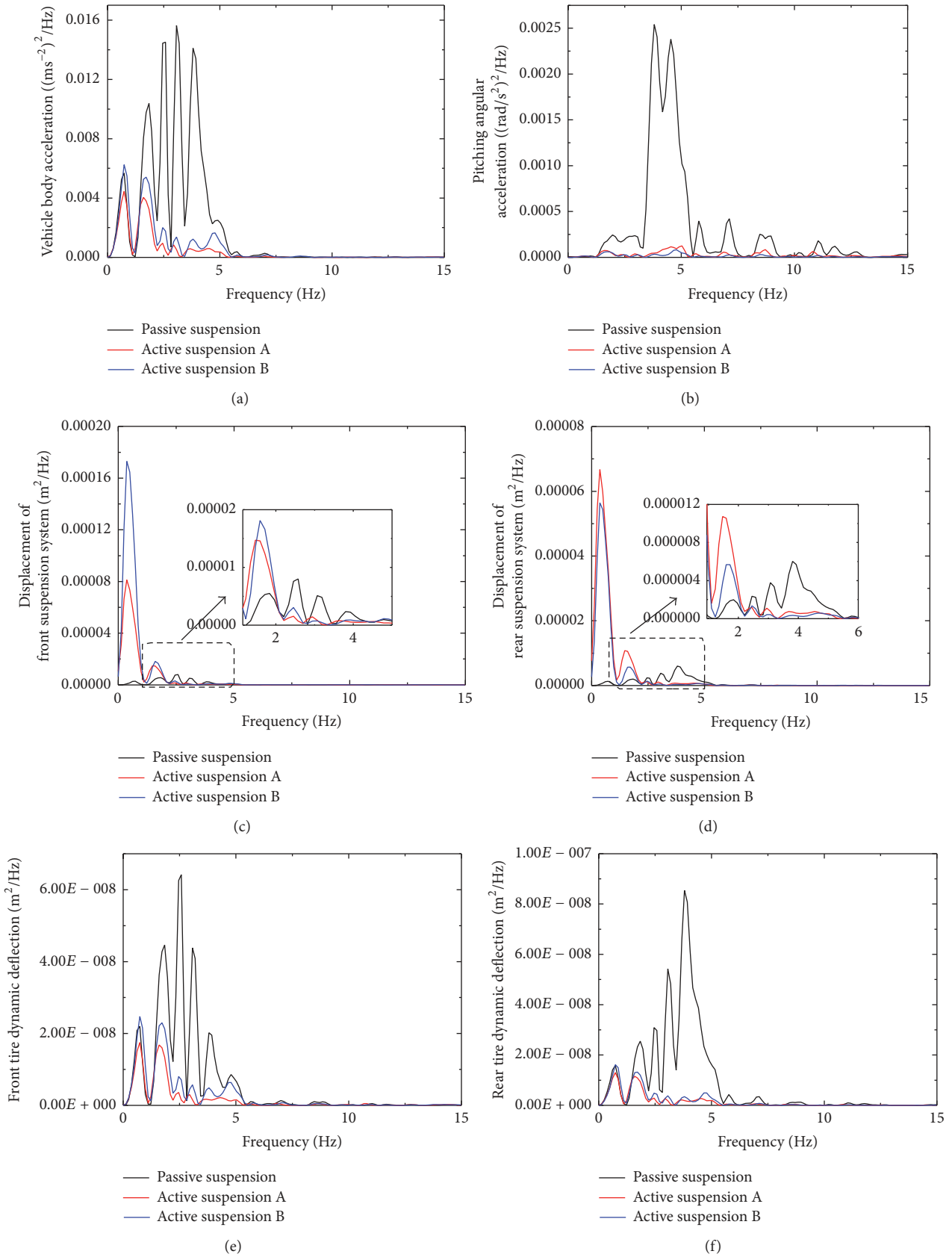φ: Pitching angle of vehicle body around y-axis

Figure 6: The PSD response to passive suspension, active suspension A, and active suspension B.

a: Distance from the front axle to CG
b: Distance from the rear axle to CG
u_f: Front control force
u_r: Rear control force
a_z: Vehicle body acceleration
aa_z: Pitching angular acceleration
f_{df}: Displacement of front suspension system
f_{dr}: Displacement of rear suspension system
t_{df}: Front tire dynamic deflection
t_{dr}: Rear tire dynamic deflection
f_0: Cut-off frequency of road irregularity
G_0: Coefficient of road irregularity
v_0: Vehicle speed
w_1: Road profiles of front suspension system
w_2: Road profiles of rear suspension system.

Competing Interests

The authors of this paper declare that there is no conflict of interests regarding the publication of this paper.
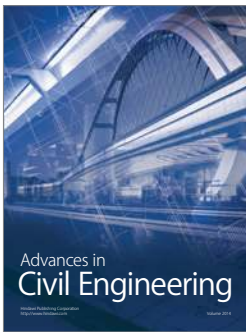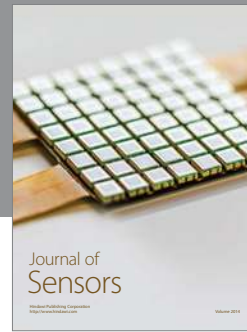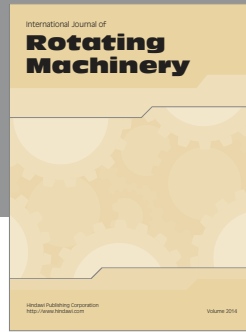
Acknowledgments

References

[1] H. Gao, J. Lam, and C. Wang, "Multi-objective control of vehicle active suspension systems via load-dependent controllers," *Journal of Sound and Vibration*, vol. 290, no. 3–5, pp. 654–675, 2006.

[2] K. Singal and R. Rajamani, "Zero-energy active suspension system for automobiles with adaptive sky-hook damping," *Journal of Vibration and Acoustics, Transactions of the ASME*, vol. 135, no. 1, 2013.

[3] L. V. V. G. Rao and S. Narayanan, "Sky-hook control of nonlinear quarter car model traversing rough road matching performance of LQR control," *Journal of Sound and Vibration*, vol. 323, no. 3–5, pp. 515–529, 2009.

[4] D. van Casteren, B. Gysen, J. Kessels, J. Paulides, P. van den Bosch, and E. Lomonova, "Non-linear full-car modeling and sky-hook control for a direct-drive active suspension system," *SAE International Journal of Passenger Cars—Mechanical Systems*, vol. 6, no. 1, pp. 252–268, 2013.

[5] H. Du and N. Zhang, "Fuzzy control for nonlinear uncertain electrohydraulic active suspensions with input constraint," *IEEE Transactions on Fuzzy Systems*, vol. 17, no. 2, pp. 343–356, 2009.

[6] J. Cao, P. Li, and H. Liu, "An interval fuzzy controller for vehicle active suspension systems," *IEEE Transactions on Intelligent Transportation Systems*, vol. 11, no. 4, pp. 885–895, 2010.

[7] M. Paksoy, R. Guclu, and S. Cetin, "Semiactive self-tuning fuzzy logic control of full vehicle model with MR damper," *Advances in Mechanical Engineering*, vol. 2014, Article ID 816813, 2014.

[8] W. Sun, H. Gao, and O. Kaynak, "Adaptive backstepping control for active suspension systems with hard constraints," *IEEE/ASME Transactions on Mechatronics*, vol. 18, no. 3, pp. 1072–1079, 2013.

[9] W. Sun, H. Pan, Y. Zhang, and H. Gao, "Multi-objective control for uncertain nonlinear active suspension systems," *Mechatronics*, vol. 24, no. 4, pp. 318–327, 2014.

[10] R.-J. Wai, J.-X. Yao, and J.-D. Lee, "Backstepping fuzzy-neural-network control design for hybrid maglev transportation system," *IEEE Transactions on Neural Networks and Learning Systems*, vol. 26, no. 2, pp. 302–317, 2015.

[11] N. Yagiz and Y. Hacioglu, "Backstepping control of a vehicle with active suspensions," *Control Engineering Practice*, vol. 16, no. 12, pp. 1457–1467, 2008.

[12] L.-H. Zong, X.-L. Gong, C.-Y. Guo, and S.-H. Xuan, "Inverse neuro-fuzzy MR damper model and its application in vibration control of vehicle suspension system," *Vehicle System Dynamics*, vol. 50, no. 7, pp. 1025–1041, 2012.

[13] D. P. Looze, "Structure of LQG controllers based on a hybrid adaptive optics system model," *European Journal of Control*, vol. 17, no. 3, pp. 237–248, 2011.

[14] A. Unger, F. Schimmack, B. Lohmann, and R. Schwarz, "Application of LQ-based semi-active suspension control in a vehicle," *Control Engineering Practice*, vol. 21, no. 12, pp. 1841–1850, 2013.

[15] T. Asami and O. Nishihara, "Closed-form exact solution to H_∞ optimization of dynamic vibration absorbers (application to different transfer functions and damping systems)," *Journal of Vibration and Acoustics*, vol. 125, no. 3, pp. 398–405, 2003.

[16] W. Wu, G. Jiang, S. Huang, and C. J. Leo, "Vertical dynamic response of pile embedded in layered transversely isotropic soil," *Mathematical Problems in Engineering*, vol. 2014, Article ID 126916, 12 pages, 2014.

[17] L. Chai and T. Sun, "The design of LQG controller for active suspension based on analytic hierarchy process," *Mathematical Problems in Engineering*, vol. 2010, Article ID 701951, 19 pages, 2010.

[18] S. Chen, H. Zhou, H. Liu, and M. Yao, "Optimal design of active suspension based on LQG control without road input signal," in *Proceedings of the 4th International Conference on Intelligent Computation Technology & Automation (ICICTA '11)*, pp. 456–459, IEEE, Shenzhen, China, March 2011.

[19] C. Li, M. Liang, Y. Wang, and Y. Dong, "Vibration suppression using two-terminal flywheel. Part II: application to vehicle passive suspension," *Journal of Vibration and Control*, vol. 18, no. 9, pp. 1353–1365, 2012.

[20] H. Y. Hu and Z. H. Wang, *Dynamics of controlled mechanical systems with delayed feedback*, Springer Berlin Heidelberg, 2002.

[21] H. Habibullah, H. R. Pota, I. R. Petersen, and M. S. Rana, "Tracking of triangular reference signals using LQG controllers for lateral positioning of an AFM scanner stage," *IEEE/ASME Transactions on Mechatronics*, vol. 19, no. 4, pp. 1105–1114, 2014.

[22] K. S. Grewal, R. Dixon, and J. Pearson, "LQG controller design applied to a pneumatic stewart-gough platform," *International Journal of Automation and Computing*, vol. 9, no. 1, pp. 45–53, 2012.

[23] H. Li, C. Y. Tang, and T. X. Zhang, "Controller of vehicle active suspension systems using LQG method," in *Proceedings of the IEEE International Conference on Automation and Logistics (ICAL '08)*, pp. 401–404, Chindao, China, September 2008.

[24] R.-X. Xia, J.-H. Li, J. He, D.-F. Shi, and Y. Zhang, "Linear-quadratic-Gaussian controller for truck active suspension based on cargo integrity," *Advances in Mechanical Engineering*, vol. 7, no. 12, Article ID 15620320, 9 pages, 2015.

[25] D. Whitley, "An Executable Model of a Simple Genetic Algorithm," vol. 2 of *Foundations of Genetic Algorithms*, pp. 45–62, Elsevier, 1993.

[26] A. Arabali, M. Ghofrani, M. Etezadi-Amoli, M. S. Fadali, and Y. Baghzouz, "Genetic-algorithm-based optimization approach for energy management," *IEEE Transactions on Power Delivery*, vol. 28, no. 1, pp. 162–170, 2013.

[27] H. Li, J. Yu, C. Hilton, and H. Liu, "Adaptive sliding-mode control for nonlinear active suspension vehicle systems using T–S fuzzy approach," *IEEE Transactions on Industrial Electronics*, vol. 60, no. 8, pp. 3328–3338, 2013.